



# Measuring and modeling evapotranspiration of a *Populus euphratica* forest in northwestern China

Guanlong Gao<sup>1,2,3</sup> · Qi Feng<sup>3</sup> · Xiande Liu<sup>4</sup> ·  
Yonghua Zhao<sup>2</sup>

Received: 2 April 2020 / Accepted: 8 July 2020 / Published online: 29 October 2020  
© Northeast Forestry University 2020

**Abstract** Vegetation is sparsely distributed in the arid regions of northwestern China, and accurately measuring and partitioning of evapotranspiration is of importance for ecosystems in such areas. In this study, we measured and analyzed diurnal and phenological variations in evapotranspiration using the eddy–covariance method based on the Penman–Monteith, Priestley–Taylor, Shuttleworth–Wallace models, a newly proposed improved dual source model and a clumped model in a forest reserve in the Ejina oasis of *Populus euphratica* in 2015 and 2016 growing seasons. A sensitivity analysis was performed for the models with higher accuracies and we examined the biotic and abiotic controls on evapotranspiration. The results show that the total amounts of evapotranspiration during the two growing

seasons in 2015 and 2016 were 622 and 612 mm, respectively. Phenological variations in evapotranspiration produced single-peak curves, while diurnal variations reflected the influence of high temperatures on some afternoons. The Priestley–Taylor and the improved dual source models gave the most accurate evapotranspiration values at the daily scale and appeared to be most suitable for the estimation of evapotranspiration for the species in arid regions. In addition, both models were the most sensitive to net radiation ( $R_n$ ).

**Keywords** Evapotranspiration · Eddy–covariance · *Populus euphratica* · Northwestern China

**Project funding:** This work was supported financially by the Shanxi Province Science Foundation for Youth (201801D221286) the Chinese Post-doctoral Science Foundation (2018M643769) the Scientific and Technological Innovation Programs of Higher Education Institutions in Shanxi (2020L0028) the Fundamental Research Funds for the Central Universities CHD (300102279505) and the Shaanxi Key Laboratory of Land Consolidation (2018–JC13).

The online version is available at <http://www.springerlink.com>.

Corresponding editor: Zhu Hong.

**Electronic supplementary material** The online version of this article (<https://doi.org/10.1007/s11676-020-01228-1>) contains supplementary material, which is available to authorized users.

✉ Yonghua Zhao  
yonghuaz@chd.edu.cn

<sup>1</sup> College of Environment and Resource, Shanxi University, Taiyuan 030006, People's Republic of China

<sup>2</sup> Shaanxi Key Laboratory of Land Consolidation, Chang'an University, Xi'an 710064, People's Republic of China

## Introduction

Dryland biomes cover approximately 41.5% of the Earth's land surface (Bastin et al. 2017). In such areas, evapotranspiration (ET), including canopy transpiration ( $E_c$ ) and soil evaporation ( $E_s$ ) (Maxwell and Condon 2016), is the key component of water cycles and energy balance (Oki and Kanae 2006; Hu et al. 2009; Jung et al. 2010; Villagarcía et al. 2010; Wei et al. 2013; Li et al. 2018), and plays a strategic role in climatology, hydrology, ecology, agriculture, and forestry (Guan and Wilson 2009; Liu et al. 2012). Knowledge of ET variations is crucial for understanding the interactions between different vegetation covers and the atmosphere (Keane et al. 2002), for better managing water

<sup>3</sup> Cold and Arid Regions Environmental and Engineering Research Institute, Chinese Academy of Sciences, Lanzhou 730000, People's Republic of China

<sup>4</sup> Academy of Water Resources Conservation Forests in Qilian Mountains of Gansu Province, Zhangye 734000, People's Republic of China

resources (Li et al. 2019), and for assessing the phenomenon of drought and its associated environmental impacts (Yu et al. 2018).

ET and its components have been measured by various expensive and labor-intensive methods (Gasca-Tucker et al. 2007), including sap flow (Williams et al. 2004; Scott et al. 2006; Juhász and Hrotkó 2014; Rafi et al. 2019), lysimeters (Zhang et al. 2005; Peters et al. 2017; Widmoser and Wohlfahrt 2018; Xu et al. 2018), stable isotopes (Yepez et al. 2003; Lu et al. 2017; Wei et al. 2018; Ma and Song 2019), the Bowen-ratio energy balance method (Zeggaf et al. 2007; Uddin et al. 2013; Comunian et al. 2018; Maruyama et al. 2019), and the eddy-covariance (EC) system (Griffis et al. 2008, 2010; Sturm et al. 2012; Zhu et al. 2012, 2013; Gao et al. 2016b; Spinelli et al. 2017; Dzikitia et al. 2018; Anapalli et al. 2020). However, these approaches focus on the direct measurement of ET flux which sometimes makes it difficult for wide application because of their high cost, complex equipment placement and validation process. Numerical simulation is a good supplement because of its applicability over a wide range of time scales and because modeling is applied to a spatial scale of an entire ecosystem (Wang et al. 2016). Numerous models, from single climatic variable-driven equations to energy balance and aerodynamic combination methods, have been developed and are becoming more popular.

The Ejin oasis, located in the lower reach of the Heihe River Basin, is in a typically arid region. Natural conditions are extremely poor, and water is the driving force of ecological evolution. The Euphrates or desert poplar, *Populus euphratica* Oliv., is the foundation species of the desert riparian forest in this region, and the *P. euphratica* forest is an important natural barrier to support the existence of the Ejin oasis. The choice of the most appropriate method for measuring and estimating the actual evapotranspiration helps to understand the water balance of *P. euphratica* and can serve for the rational use of water resources, and for the protection and stability of the *P. euphratica* forest ecosystem (Hou et al. 2010). In this study, ET of a *P. euphratica* forest was estimated using five models: the Penman–Monteith (PM) model, the Priestley–Taylor (PT) model, the Shuttleworth–Wallace (SW) model, an improved dual source (SSW) model and a clumped (C) model. The accuracy of each was verified by the EC measured data. The five models were selected for the following reasons:

(1) The Penman–Monteith (PM) model treats the crop canopy as a single uniform cover but neglects evaporation from the soil surface and may be inappropriate for sparsely vegetated canopies (Mo 1998). In this study, the accuracy of the PM model was tested for the sparse *P. euphratica* forest canopy; (2) The Priestley–Taylor (PT) model, with an appropriately defined empirical parameter ( $\alpha$ ) value, performed remarkably well despite its relative simplicity; (3) The

Shuttleworth–Wallace (SW) model has been validated and found suitable for estimating evapotranspiration from fragmented canopies (Guan and Wilson 2009; Hu et al. 2013). Researchers have now mainly focused on improving the SW accuracy under specific conditions; however, the complexity and number of parameters also have been increased; (4) The improved dual source (SSW) model proposed by Li et al. (2010), has a simpler structure, fewer parameters and only requires conventional meteorological data. The applicability, however, requires testing in different natural ecosystems with variable vegetation types and conditions; and, (5) the clumped (C) model partitions energy among vegetation and soil based on fractional vegetative cover ( $f$ ), and its theory is more reasonable compared to those of single- and two-layer models. But the model requires a large number of parameters and determination of these parameters is rather difficult, leading to increased model error (Zhang et al. 2008). Application of the C model is rare due to its complexity; however, it was tested here for further research. As previous studies modeling ET of *P. euphratica* have mainly focused on a single model (Wang et al. 2014; Gao et al. 2016a; Yu et al. 2017), our research will be of significance as the measuring, modeling and partitioning of ET of a *P. euphratica* forest in the Ejin oasis has not been reported.

## Materials and methods

### Study area

The research was carried out in a 13.3 km<sup>2</sup> area of the Qidaoqiao *P. euphratica* forest reserve in Ejin County, Inner Mongolia, China (42° 21' N, 101° 15' E, altitude 920.5 m a.s.l.). This region is extremely arid and evaporation exceeds 3600 mm year<sup>-1</sup> and the mean annual rainfall is 36.5 mm (Fig. 1). Mean annual air temperature is

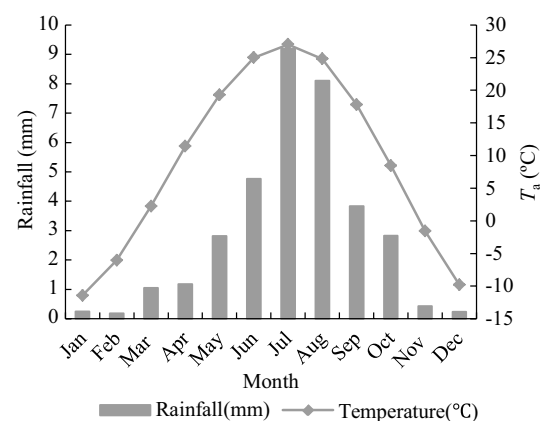


**Fig. 1** Mean monthly rainfall and mean air temperatures from 1960 to 2016 at the study site

9.5 °C and mean annual relative humidity is 36–44%. In the forest reserve, average tree height is 10.4 m, average age 35 years, average diameter at breast height 24.8 cm, and average crown breadth 452 cm × 480 cm. The saturated soil water content is 22.05 g cm<sup>-3</sup> and bulk density 1.72 g cm<sup>-3</sup>.

### Flux and meteorological measurements

A uniform open-path eddy-covariant (EC) system and meteorological instruments were installed in a tower to monitor CO<sub>2</sub>/H<sub>2</sub>O fluxes and environmental conditions at 20 m and 10 m, respectively. The tower was located in the center of the *P. euphratica* forest and the trees were distributed evenly around the tower. The fetch of the EC system was approximately 1000 m in the predominant upwind direction. The EC system consisted of a 3D sonic anemometer/thermometer (model CSAT3, Campbell Scientific Inc., Logan, UT, USA) and an open-path CO<sub>2</sub>/H<sub>2</sub>O gas analyzer (model LI-7500, Li-COR Inc., Lincoln, NE, USA). Signals were recorded by a datalogger (model CR3000, Campbell Scientific, Logan, UT, USA) and block-averaged over 30 min intervals.

Meteorological variables were measured simultaneously with the EC data. Rainfall was measured using a rain gauge (RG3-M, Onset Co., Bourne, MA, USA). Net radiation ( $R_n$ , W m<sup>-2</sup>) and photosynthetic active radiation (PAR; W m<sup>-2</sup>) were measured 10-m above ground by radiometers (model CNR-4, Kipp and Zonen, Delft, The Netherlands; LI-190SA, LI-COR Inc., Lincoln, NE, USA). Air temperature ( $T_a$ ; °C) and relative humidity (RH; %) were measured 10-m above ground (model HMP45C, Campbell Scientific, Logan, UT, USA). Barometric pressure ( $P_a$ ; kPa) was measured by shielded and aspirated probes. Soil temperature ( $T_s$ , °C) (109SS, Campbell Scientific, Logan, UT, USA) and volumetric water content ( $\theta$ ; %) (SMC300, Spectrum Technologies, Plainfield, USA) were measured at depths of 10, 30, 50, 80 and 150 cm. The groundwater depth (GWD, m) was measured automatically by pressure transducers (HOBO-U20, Onset Computer Corporation, Bourne, MA, USA) at 0.5 h intervals. Soil heat flux ( $G$ , W m<sup>-2</sup>) was measured at a 5 cm depth by two buried flux plates (model HFP01SC, Campbell Scientific, Logan, UT, USA) – one in soil under vegetation and the other in bare soil between vegetation.

Leaf area index (LAI; m<sup>2</sup> m<sup>-2</sup>) was measured once a month from May through October using a plant canopy analyzer (LAI2200, LI-COR Inc., Lincoln, NE, USA) under diffuse light conditions at dawn or dusk. A 10° view cap was used for each LAI recorded, and four readings above the canopy and eight other readings at different points within 1 m of each other at the base of the canopy were taken. Fractional vegetative cover ( $f$ ) was estimated every month by measuring the canopy dimensions.

### Data processing

CO<sub>2</sub>/H<sub>2</sub>O flux and CSAT3 data were processed using Eddy-Pro software (LI-COR Biosciences, Inc., Lincoln, NE, USA) and included block average detrending, time lag compensation by covariance maximization (with default), double coordinate rotation, and density fluctuation compensation by the use/convert feature to the mixing ratio. Statistical analysis of the raw time series data was processed according to Vickers and Mahrt (1997), and quality check flagging was obtained according to the CarboEurope standard.

To obtain accurate ET estimates, data from the measurements were filtered to eliminate errors. Night-time data was first eliminated with  $R_n < 10$  W m<sup>-2</sup> (to include dusk and dawn moments) as turbulent transport diminishes during night-time stable atmospheric conditions. Total ET values > 800 W m<sup>-2</sup> was also eliminated according to limits proposed by CarboEurope (Villagarcía et al. 2010). The energy balance was also analyzed for the flux data (80.9% in 2015 and 82.6% in 2016, Fig. 2). The latent heat data (LE, W m<sup>-2</sup>) of energy unbalance were removed. Gap-filling was conducted when total ET was calculated. Small gaps of less than 2 h were filled by linear interpolation, while longer gaps were filled using the energy balance (Falge et al. 2001; Zhu et al. 2014). The evapotranspiration models were evaluated using daytime (8:00–19:00 h) averages as nighttime measurements were unreliable. Sample sizes were both 158 daytime averages based on 1896 measurements in 2015 and 2016.

### Data analysis

The 2015 and 2016 growing seasons were divided into four phenological growth periods according to Zhang et al. (2007): leaf expansion period (May 4th–12th), fruit expansion period

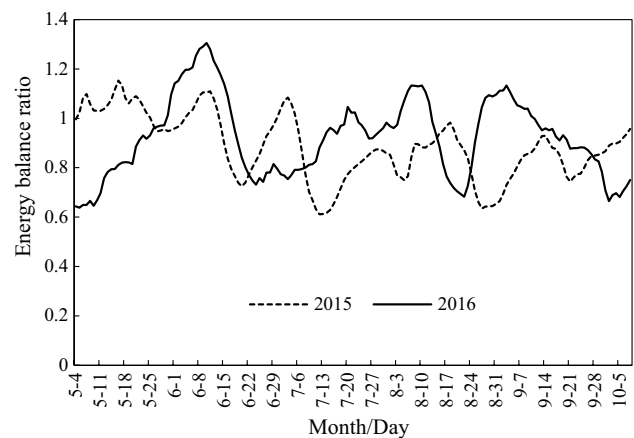


**Fig. 2** Energy balance ratios during the *Populus euphratica* growing seasons in 2015 and 2016

(May 13th–Jul 27th), seed dispersal period (Jul 28th–Sep 30th) and leaf discoloration period (Oct 1st–8th). Pearson’s correlation was applied to examine correlations between ET and environmental variables. All statistical analyses and plotting were performed with the SPSS Statistics software (Version 19.0; IBM, Armonk, NY, USA) and Origin (Version 8.0; OriginLab, Northampton, MA, USA).

**Expressions of the models**

The Penman–Monteith (PM) model is expressed as (Monteith 1965):

$$\lambda ET = \frac{\Delta(R_n - G) + (\rho C_p D / r_a)}{\Delta + \gamma(1 + (r_c / r_a))} \tag{1}$$

where ET is evapotranspiration (mm d<sup>-1</sup>), r<sub>c</sub> is surface canopy resistance (s m<sup>-1</sup>), r<sub>a</sub> is aerodynamic resistance (s m<sup>-1</sup>), R<sub>n</sub> is net radiation (W m<sup>-2</sup>), G is soil heat flux (W m<sup>-2</sup>), ρ is air density (kg m<sup>-3</sup>), C<sub>p</sub> is specific heat at constant pressure (J kg<sup>-1</sup> K<sup>-1</sup>), D is vapor pressure deficit in the air (kPa), Δ is slope of the saturated vapor pressure versus temperature curve (kPa K<sup>-1</sup>), γ is psychrometric constant (kPa K<sup>-1</sup>), λ is the latent heat of vaporization (J kg<sup>-1</sup>).

Owing to the frequent unavailability of some micrometeorological variables needed for this model, Priestley and Taylor (1972) proposed the Priestley–Taylor (PT) model, a simplified version to calculate ET:

$$\lambda ET = \alpha \frac{\Delta}{\Delta + \gamma} (R_n - G) \tag{2}$$

where ET is evapotranspiration (mm d<sup>-1</sup>), R<sub>n</sub> is net radiation (W m<sup>-2</sup>), G is soil heat flux (W m<sup>-2</sup>), Δ is slope of the saturated vapor pressure versus temperature curve (kPa K<sup>-1</sup>), γ is psychrometric constant (kPa K<sup>-1</sup>), λ is the latent heat of vaporization (J kg<sup>-1</sup>), α is Priestley–Taylor coefficient.

The Shuttleworth–Wallace (SW) model estimates latent heat flux from the canopy and soil surface as two distinct sources and calculates ecosystem ET as the sum of E<sub>c</sub> and E<sub>s</sub>:

$$\lambda ET = \lambda E_c + \lambda E_s = C_c PM_c + C_s PM_s \tag{3}$$

$$E_s = \alpha_E \tau \frac{\Delta}{\lambda(\Delta + \gamma)} (R_n - G) \begin{cases} \tau \ll \tau_c, \alpha_E = 1 \\ \tau > \tau_c, \alpha_E = \alpha - (\alpha - 1)(1 - \tau)(1 - \tau_c) \end{cases} \tag{13}$$

$$PM_s = \frac{\Delta A_c + [\rho C_p D - \Delta r_a^s (A_c - A_s)] / (r_a^a + r_a^s)}{\Delta + \gamma \left[ 1 + \frac{r_s^s}{r_a^a + r_a^s} \right]} \tag{4}$$

$$PM_c = \frac{\Delta A_c + [\rho C_p D - \Delta r_a^c A_s] / (r_a^a + r_a^c)}{\Delta + \gamma \left[ 1 + \frac{r_s^c}{r_a^a + r_a^c} \right]} \tag{5}$$

$$A_c = R_n - G \tag{6}$$

$$A_s = R_{ns} - G \tag{7}$$

$$C_s = \frac{R_c (R_s + R_a)}{R_s R_c + R_c R_a + R_s R_a} = \frac{1}{1 + \frac{R_s R_a}{R_c (R_s + R_a)}} \tag{8}$$

$$C_c = \frac{R_s (R_c + R_a)}{R_s R_c + R_c R_a + R_s R_a} = \frac{1}{1 + \frac{R_c R_a}{R_s (R_c + R_a)}} \tag{9}$$

$$R_a = (\Delta + \gamma) r_a^a \tag{10}$$

$$R_c = (\Delta + \gamma) r_a^c + \gamma r_s^c \tag{11}$$

$$R_s = (\Delta + \gamma) r_a^s + \gamma r_s^s \tag{12}$$

where ET is evapotranspiration (mm d<sup>-1</sup>), E<sub>c</sub> is canopy transpiration (mm d<sup>-1</sup>), E<sub>s</sub> is soil evaporation (mm d<sup>-1</sup>), C<sub>i</sub> is resistance coefficient of i source (c and s), PM<sub>i</sub> is Penman–Monteith–type equations for each i source (c and s), A<sub>i</sub> is available energy for each i source (c and s) (W m<sup>-2</sup>), R<sub>n</sub> is net radiation (W m<sup>-2</sup>), R<sub>ns</sub> is net radiation for soil (W m<sup>-2</sup>), G is soil heat flux (W m<sup>-2</sup>), r<sub>a</sub><sup>a</sup> is aerodynamic resistance between the canopy source height and reference level (s m<sup>-1</sup>), r<sub>a</sub><sup>s</sup> is aerodynamic resistance between the soil and canopy source height (s m<sup>-1</sup>), r<sub>a</sub><sup>c</sup> is bulk boundary layer resistance of the vegetative elements in the canopy (s m<sup>-1</sup>), r<sub>s</sub><sup>c</sup> is canopy resistance (s m<sup>-1</sup>), r<sub>s</sub><sup>s</sup> is soil surface resistance (s m<sup>-1</sup>), ρ is air density (kg m<sup>-3</sup>), C<sub>p</sub> is specific heat at constant pressure (J kg<sup>-1</sup> K<sup>-1</sup>), D is vapor pressure deficit in the air (kPa), Δ is slope of the saturated vapor pressure versus temperature curve (kPa K<sup>-1</sup>), γ is psychrometric constant (kPa K<sup>-1</sup>), λ is the latent heat of vaporization (J kg<sup>-1</sup>).

The simpler structure of the improved dual source (SSW) model with its fewer parameters can also estimate E<sub>c</sub> and E<sub>s</sub> separately and only requires conventional meteorological data (Li et al. 2010). The equations are:

$$E_c = \frac{1}{\lambda} \frac{\Delta R_{nc} + (\rho C_p D / r_a^c) + \Delta (1 - \alpha_E \tau) (R_n - G) (r_a^a / r_a^c)}{\Delta + \gamma (1 + (r_s^c / r_a^c)) + (\Delta + \gamma) (r_a^a / r_a^c)} \tag{14}$$

where E<sub>c</sub> is canopy transpiration (mm d<sup>-1</sup>), E<sub>s</sub> is soil evaporation (mm d<sup>-1</sup>), R<sub>n</sub> is net radiation (W m<sup>-2</sup>), R<sub>nc</sub> is net radiation for canopy (W m<sup>-2</sup>), G is soil heat flux (W m<sup>-2</sup>),

$r_a^a$  is aerodynamic resistance between the canopy source height and reference level ( $s\ m^{-1}$ ),  $r_a^c$  is bulk boundary layer resistance of the vegetative elements in the canopy ( $s\ m^{-1}$ ),  $r_s^c$  is canopy resistance ( $s\ m^{-1}$ ),  $\rho$  is air density ( $kg\ m^{-3}$ ),  $C_p$  is specific heat at constant pressure ( $J\ kg^{-1}\ K^{-1}$ ),  $D$  is vapor pressure deficit in the air (kPa),  $\Delta$  is slope of the saturated vapor pressure versus temperature curve ( $kPa\ K^{-1}$ ),  $\gamma$  is psychrometric constant ( $kPa\ K^{-1}$ ),  $\lambda$  is the latent heat of vaporization ( $J\ kg^{-1}$ ),  $\alpha_E$  is coefficient of PT formula with relevance to light interception,  $\alpha$  is Priestley–Taylor coefficient,  $\tau_c$  is constant value at which the leaf area index is sufficient for  $\alpha_E$  to reach unity.

The clumped (C) model considers three evaporating sources, vegetation (p), soil under vegetation (s) and bare soil between vegetation (bs); the energy available for ET is distributed among the three sources (Villagarcía et al. 2010). Thus, total ET can be calculated as:

$$\lambda ET = \lambda T + \lambda E^s + \lambda E^{bs} = f(C_c^s PM_c^s + C_c^p PM_c^p) + (1 - f)C_c^{bs} PM_c^{bs} \tag{15}$$

$$PM_c^p = \frac{\Delta A_c + [(\rho C_p D - \Delta r_a^c A_c^s) / (r_a^a + r_a^c)]}{\Delta + \gamma [1 + r_s^c / (r_a^a + r_a^c)]} \tag{16}$$

$$PM_c^{bs} = \frac{\Delta A_c^{bs} + [(\rho C_p D - r_a^s A_c^p) / (r_a^a + r_a^{bs})]}{\Delta + \gamma [1 + r_s^{bs} / (r_a^a + r_a^{bs})]} \tag{17}$$

$$PM_c^{bs} = \frac{\Delta A_c^{bs} + [\rho C_p D / (r_a^a + r_a^{bs})]}{\Delta + \gamma [1 + r_s^{bs} / (r_a^a + r_a^{bs})]} \tag{18}$$

$$C_c^s = R_c^{bs} R_c^p (R_c^s + R_c^a) / [R_c^s R_c^p R_c^{bs} + (1 - f)R_c^s R_c^p R_c^a + fR_c^{bs} R_c^s R_c^a + fR_c^{bs} R_c^p R_c^a] \tag{19}$$

$$C_c^p = R_c^{bs} R_c^s (R_c^p + R_c^a) / [R_c^s R_c^p R_c^{bs} + (1 - f)R_c^s R_c^p R_c^a + fR_c^{bs} R_c^s R_c^a + fR_c^{bs} R_c^p R_c^a] \tag{20}$$

$$C_c^{bs} = R_c^s R_c^p (R_c^{bs} + R_c^a) / [R_c^s R_c^p R_c^{bs} + (1 - f)R_c^s R_c^p R_c^a + fR_c^{bs} R_c^s R_c^a + fR_c^{bs} R_c^p R_c^a] \tag{21}$$

$$R_c^s = (\Delta + \gamma)r_a^s + \gamma r_s^c \tag{22}$$

$$R_c^p = (\Delta + \gamma)r_a^c + \gamma r_s^c \tag{23}$$

$$R_c^{bs} = (\Delta + \gamma)r_a^{bs} + \gamma r_s^{bs} \tag{24}$$

$$R_c^a = (\Delta + \gamma)r_a^a \tag{25}$$

where ET is evapotranspiration ( $mm\ d^{-1}$ ),  $E_c$  is canopy transpiration ( $mm\ d^{-1}$ ),  $E_s$  is soil evaporation ( $mm\ d^{-1}$ ),  $C_i$  is

resistance coefficient of  $i$  source (c, s and bs),  $PM_i$  is Penman–Monteith–type equations for each  $i$  source (c, s and bs),  $A_i$  is available energy for each  $i$  source (c and bs) ( $W\ m^{-2}$ ),  $r_a^a$  is aerodynamic resistance between the canopy source height and reference level ( $s\ m^{-1}$ ),  $r_a^s$  is aerodynamic resistance between the soil and canopy source height ( $s\ m^{-1}$ ),  $r_a^c$  is bulk boundary layer resistance of the vegetative elements in the canopy ( $s\ m^{-1}$ ),  $r_s^c$  is canopy resistance ( $s\ m^{-1}$ ),  $r_s^s$  is soil surface resistance ( $s\ m^{-1}$ ),  $\rho$  is air density ( $kg\ m^{-3}$ ),  $C_p$  is specific heat at constant pressure ( $J\ kg^{-1}\ K^{-1}$ ),  $D$  is vapor pressure deficit in the air (kPa),  $\Delta$  is slope of the saturated vapor pressure versus temperature curve ( $kPa\ K^{-1}$ ),  $\gamma$  is psychrometric constant ( $kPa\ K^{-1}$ ),  $\lambda$  is the latent heat of vaporization ( $J\ kg^{-1}$ ),  $f$  is fractional vegetative cover (%).

### Determination of parameters

Parameters of the five ET models are calculated according to:

$$r_a = \frac{\ln((z - d)/(h - d)) \ln((z - d)/z_0)}{uk^2} \tag{26}$$

$$r_c = r_a \left( a \frac{r^*}{r_a} + b \right) \tag{27}$$

$$r^* = \frac{\Delta + \gamma}{\Delta} \frac{\rho C_p D}{\gamma (R_n - G)} \tag{28}$$

$$R_{ns} = R_n \exp(-kLAI) \tag{29}$$

$$R_{nc} = R_n (1 - \exp(-kLAI)) \tag{30}$$

$$A_c = R_n - [fG_s + (1 - f)G_{bs}] \tag{31}$$

$$A_c^p = R_n - R_{ns} \tag{32}$$

$$A_c^s = R_{ns} - G_s \tag{33}$$

$$A_c^{bs} = R_n - G_{bs} \tag{34}$$

$$\Delta = \frac{4098 \left[ 0.6108 \exp \left( \frac{17.27T_a}{T_a + 237.3} \right) \right]}{(T_a + 237.3)^2} \tag{35}$$

$$r_s^s = c\theta^e \tag{36}$$

$$r_a^c = r_b \sigma_b / LAI \tag{37}$$

$$r_b = \frac{100}{n} \frac{\sqrt{w/u_h}}{1 - \exp(-n/2)} \tag{38}$$

$$n = \begin{cases} 2.5, & h_c \ll 1 \\ 2.306 + 0.194h_c, & 1 < h_c < 10 \\ 4.25, & h_c \gg 10 \end{cases} \tag{39}$$

$$r_a^a = \frac{LAI}{4} r_a^a(\alpha) + \frac{(4 - LAI)}{4} r_a^a(0) \tag{40}$$

$$r_a^s = \frac{LAI}{4} r_a^s(\alpha) + \frac{(4 - LAI)}{4} r_a^s(0) \tag{41}$$

$$r_a^s(0) = \frac{\ln \left( \frac{z}{z'_0} \right) \ln \left\{ \frac{(d+z_0)}{z'_0} \right\}}{uk^2} \tag{42}$$

$$r_a^a(0) = \frac{\ln \left( \frac{z}{z'_0} \right) \ln \left( \frac{z}{z'_0} \right)}{uk^2} - r_a^s(0) \tag{43}$$

$$r_a^a(\alpha) = \frac{\ln \left( \frac{z-d}{z_0} \right)}{uk^2} \frac{h}{n(h-d)} \times \left[ \exp n - \exp \left[ n \left\{ 1 - \frac{(d+z_0)}{h} \right\} \right] \right] \tag{44}$$

$$r_a^a(\alpha) = \frac{\ln \left( \frac{z-d}{z_0} \right)}{uk^2} \left[ \ln \left\{ \frac{(z-d)}{h-d} \right\} + \frac{h}{n(h-d)} \times \left[ \exp \left[ n \left\{ 1 - \frac{(d+z_0)}{h} \right\} \right] - 1 \right] \right] \tag{45}$$

$$r_a^{bs} = \ln \frac{(z_m/z'_0)^2}{(k^2 u_m)} \tag{46}$$

$$d = 1.1h \ln \left( 1 + (C_d LAI)^{0.25} \right) \tag{47}$$

$$z_0 = z'_0 + 0.3h(C_d LAI)^{0.5} \tag{48}$$

$$z'_0 = 0.01h \tag{49}$$

$$z_m = 0.75h \tag{50}$$

$$u = u_z \frac{4.87}{\ln(67.8z - 5.42)} \tag{51}$$

$$u_h = \frac{\ln \left[ (h-d)/z_0 \right]}{\ln \left[ (z-d)/z_0 \right]} u_z \tag{52}$$

$$r_s^c = \left\{ \frac{m(1 + gD)(i + R_s)}{R_s} \right\} \left( \frac{LAI_s}{LAI} \right) \tag{53}$$

where  $R_n$  is net radiation ( $W m^{-2}$ ),  $R_{ni}$  is net radiation for each  $i$  source (c and s),  $A_c^i$  is available energy for each  $i$  source (c, s and bs) ( $W m^{-2}$ ),  $G$  is soil heat flux ( $W m^{-2}$ ),  $G_i$  is soil heat flux for each  $i$  source (c and s) ( $W m^{-2}$ ),  $r_a^a$  is aerodynamic resistance between the canopy source height and reference level ( $s m^{-1}$ ),  $r_a^s$  is aerodynamic resistance between the soil and canopy source height ( $s m^{-1}$ ),  $r_a^c$  is bulk boundary layer resistance of the vegetative elements in the canopy ( $s m^{-1}$ ),  $r_s^c$  is canopy resistance ( $s m^{-1}$ ),  $r_s^s$  is soil surface resistance ( $s m^{-1}$ ),  $\rho$  is air density ( $kg m^{-3}$ ),  $C_p$  is specific heat at constant pressure ( $J kg^{-1} K^{-1}$ ),  $D$  is vapor pressure deficit in the air (kPa),  $\Delta$  is slope of the saturated vapor pressure versus temperature curve ( $kPa K^{-1}$ ),  $\gamma$  is psychrometric constant ( $kPa K^{-1}$ ),  $T_a$  is air temperature ( $^{\circ}C$ ),  $r_a$  is aerodynamic resistance ( $s m^{-1}$ ),  $r_c$  is surface canopy resistance ( $s m^{-1}$ ),  $r^*$  is critical resistance ( $s m^{-1}$ ),  $r_b$  is leaf boundary layer resistance ( $s m^{-1}$ ),  $z$  is reference height above the forest at which meteorological measurements are available (m),  $z_0$  is roughness length of a forest with complete canopy cover (m),  $z'_0$  is roughness length of bare soil (m),  $z_m$  is mean surface flow height (m),  $h$  is canopy height (m),  $d$

( $W\ m^{-2}$ ),  $LAI_s$  is leaf area index for which these parameters were determined ( $m^2\ m^{-2}$ ),  $a$  and  $b$  are empirical calibration coefficients,  $e$ ,  $g$ ,  $i$  and  $m$  are empirical constants,  $n$  is eddy diffusivity decay constant.

**Assessments**

The modified coefficient of efficiency ( $E_1$ ), the modified index of agreement ( $d_1$ ), and the mean absolute error ( $M_{AE}$ ) were calculated according to Legates and McCabe (1999) to characterize deviation of the calculated values from the observed:

$$E_1 = 1 - \frac{\sum_{i=1}^N |O_i - M_i|}{\sum_{i=1}^N |O_i - \bar{O}_i|}, \tag{54}$$

$$d_1 = 1 - \frac{\sum_{i=1}^N |O_i - M_i|}{\sum_{i=1}^N (|O_i - \bar{O}_i| + |M_i - \bar{O}_i|)}, \tag{55}$$

$$M_{AE} = \frac{\sum (|O_i - M_i|)}{N}. \tag{56}$$

where  $O_i$  and  $M_i$  are the observed and modeled values, respectively,  $\bar{O}_i$  is the mean observed values,  $N$  is the total number of observations.

Fitness of a model is considered good when the coefficient of determination ( $R^2$ ),  $E_1$  and  $d_1$  are high while the  $M_{AE}$  is low, and the slope between  $O_i$  and  $M_i$  is close to 1.

A simple method proposed by Zhan et al. (1996) was used to investigate the relative influence of the different parameters on model outputs:

$$S_p = \left| \frac{E_{T-} - E_{T+}}{E_{T0}} \right| \tag{57}$$

where  $E_{T0}$ ,  $E_{T-}$  and  $E_{T+}$  are ET variables derived by the model when the corresponding parameter equals its reference value, i.e.,  $P_0$ ,  $1.1 P_0$  and  $0.9 P_0$ .

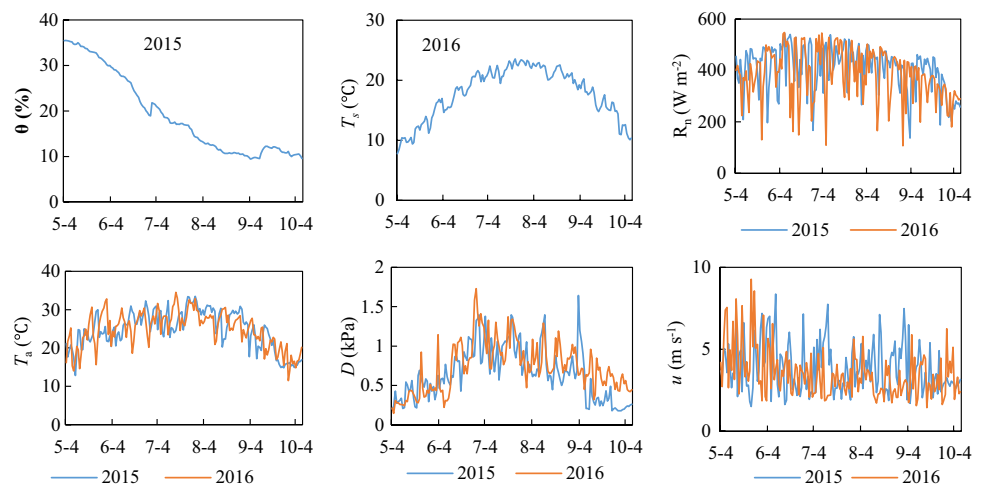
**Results**

**Environmental variables associated with ET**

Detailed information on the seasonality of key environmental variables is essential to assess seasonal variations in ET (Zhu et al. 2012). For the *P. euphratica* growing seasons, changes in the daily average  $\theta$  (volumetric water content) in 2015 and  $T_s$  (soil temperature) in 2016 (due to instrument malfunctions, data of  $\theta$  in 2016 and  $T_s$  in 2015 are missing),  $R_n$  (net radiation),  $T_a$  (air temperature),  $D$  (vapor pressure deficit) and  $u$  (wind speed) in 2015 and 2016 are illustrated in Fig. 3. The trend of  $\theta$  continuously declined, and its average measure was 19.2%, varying from 35.5 to 9.5%. Trends of  $T_s$  and  $T_a$  were similar; however, compared with the average measure of  $T_s$  (17.8 °C), corresponding values of  $T_a$  were greater (24.7 °C in 2015 and 24.8 °C in 2016). These were similar to those of the previous year (data not shown). Average measures of  $R_n$  (net radiation) were 407.8 and 384.8  $W\ m^{-2}$ , varying from 137.0 to 544.2  $W\ m^{-2}$  and 107.3 to 547.5  $W\ m^{-2}$  for 2015 and 2016, respectively. Average measures of  $u$  were ~3.8 and 3.5  $m\ s^{-1}$ , varying from 1.5 to 8.4  $m\ s^{-1}$  and 0.4 to 12.0  $m\ s^{-1}$ , respectively. Wind speeds in May and in September to October were higher than in other months, mainly due to the prevailing winds in spring and autumn. Average measures of  $D$  were ~0.6 and 0.7 kPa, ranging from 0.2 to 1.6 kPa and 0.2 to 1.7 kPa for 2015 and 2016, respectively.

The change of daily GWD (ground water depth) during the growing season of *P. euphratica* in 2016 are shown in Fig. 4. Data for GWD in 2015, similar to  $T_s$ , is missing due

**Fig. 3** Changes in daily average soil water content ( $\theta$ ) in 2015, soil temperature ( $T_s$ ) in 2016, net radiation ( $R_n$ ), air temperature ( $T_a$ ), vapor pressure deficit ( $D$ ) and wind speed ( $u$ ) during the growing seasons of *Populus euphratica* in 2015 and 2016



to the instrument malfunction. However, GWD decreased gradually to a minimum of 2.2 m on the 18th of September, after which it suddenly increased to 158 mm above ground following a flood irrigation. The course of GWD indicated that its seasonal variation was controlled by both the water uptake by the trees and by irrigation. The ground water fell after the onset of the growing season in 2016, indicating groundwater uptake by the trees, and then it increased, indicating that the water consumption by the trees was less than by irrigation.

Leaf area index (LAI) is also an important factor affecting evapotranspiration. According to the most accurate dual source SSW model, monthly  $E_c$ , ET,  $E_c/ET$  and LAI were analyzed (Fig. 5). Total  $E_c$  and ET values from May

to September were 33, 51, 68, 90 and 55 mm and 93, 112, 131, 126 and 86 mm in 2015, and 34, 19, 66, 81 and 53 mm and 85, 108, 132, 119 and 89 mm in 2016. The variation between  $E_c/ET$  and LAI was similar. From May to August in 2015 and 2016,  $E_c/ET$  increased from 36.0 to 72.1% and 39.9 to 68.5%, respectively, which corresponds to LAI changing from 1.7 to 3.2  $m^2 m^{-2}$  and 1.8 to 2.9  $m^2 m^{-2}$  for both years. From August to September in 2015 and 2016,  $E_c/ET$  decreased from 72.1 to 64.1% and 68.5 to 59.7%, respectively, which corresponds to the LAI changing from 3.2 to 2.7  $m^2 m^{-2}$  and 2.9 to 2.5  $m^2 m^{-2}$  for both years, respectively.

### Characteristics of evapotranspiration

#### Diurnal variation in ET

Diurnal variations of ET for the first 10 days during the growing season of the *P. euphratica* forest in 2015 and 2016 are shown in Fig. 6. Ten days for both years were selected as the study periods because the measured ET by the EC method for these days was the sum of  $E_c$  and  $E_s$ , without considering the influence of transpiration from surface vegetation (mostly *Sophora alopecuroides* L.), as it was not as yet growing in the *P. euphratica* forest. Evapotranspiration increased rapidly from sunrise and maximized at approximately mid-day, and then decreased. In the afternoons on some days, ET decreased slightly after noon and then fluctuated until it reached another peak around 17:00 h, due to high temperatures causing leaf stomata to close. After that, ET decreased rapidly until sunset.



**Fig. 4** Changes of daily groundwater depth (GWD) during the growing season of *Populus euphratica* in 2016

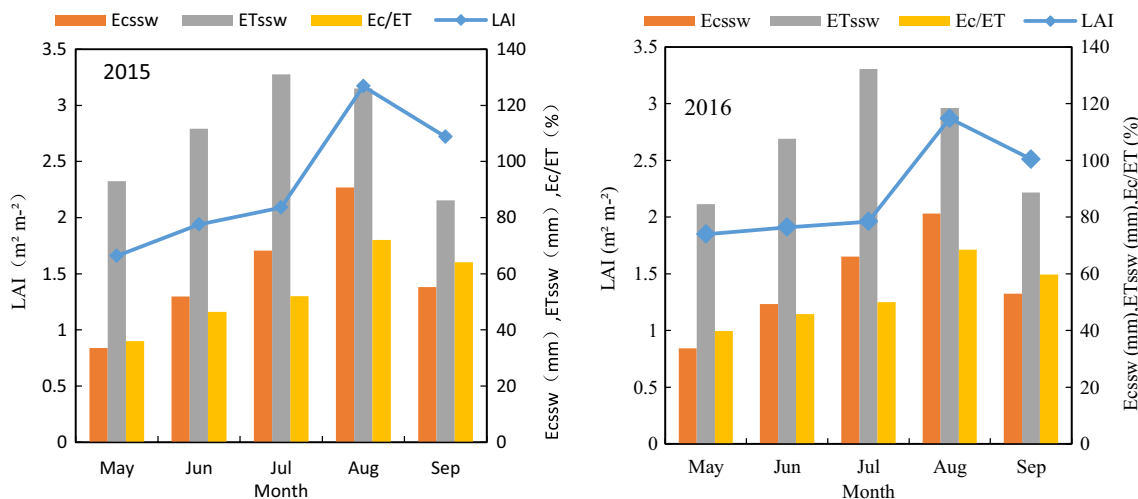
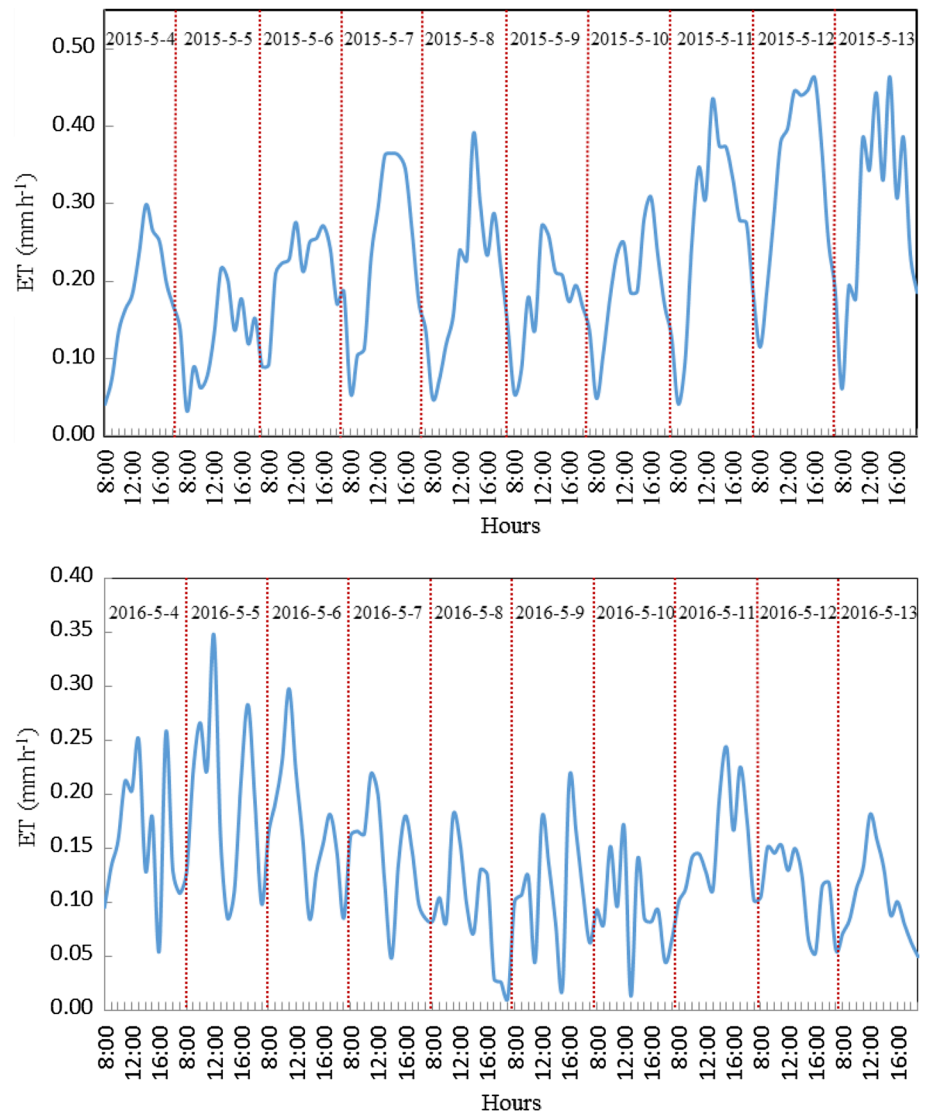


**Fig. 5** Patterns of monthly canopy transpiration ( $E_c$ ), evapotranspiration (ET) and  $E_c/ET$  from the improved dual source model (SSW) and leaf area index (LAI) during the growing season of *Populus euphratica* in 2015 and 2016



**Fig. 6** Diurnal patterns of hourly evapotranspiration measured by the eddy-covariance method on the first ten days during the growing seasons in 2015 and 2016



#### The phenological variation in evapotranspiration

The phenological variation patterns of ET during the growing seasons of the *P. euphratica* forest in 2015 and 2016 are shown in Fig. 7 and generally were single-peak curves. ET levels in 2015 and 2016 were 622 and 612 mm, respectively, with the fruit expansion period and the period of seed dispersal the major contributors; the average ET in the fruit expansion period was maximum. Total ET values in the fruit expansion period were 348 and 316 mm, accounting for 52.9% and 51.6% in 2015 and 2016, respectively. Evapotranspiration in the seed dispersal periods in 2015 and 2016 were 270 and 261 mm, respectively, slightly less than in the fruit expansion period. Average values in the leaf expansion and discolouration periods were much less, as leaves had not fully formed in the previous period and leaf activity decreased in the latter period. Total ET values in the leaf expansion periods in 2015 and 2016 were 23 mm

and 15 mm, accounting for 3.5% and 2.5%, respectively. Similarly, evapotranspiration levels in the leaf discolouration period in 2015 and 2016 were small at 16 mm and 19 mm, accounting for 2.5% and 3.1% respectively.

#### Correlations between ET and environmental variables

ET in 2015 and 2016 was positively correlated to all the environmental variables except for volumetric water content ( $\theta$ ), and significantly correlated to net radiation ( $R_n$ ) in both years (0.803 in 2015 and 0.819 in 2016) but not significantly correlated to wind speed ( $u$ ) (Table 1). Except for net radiation, ET was also positively correlated to air temperature ( $T_a$ ) and vapour pressure ( $D$ ), with Pearson's correlation coefficients of 0.752 and 0.776 for air temperature and 0.732 and 0.721 for vapour pressure for 2015 and 2016, respectively.

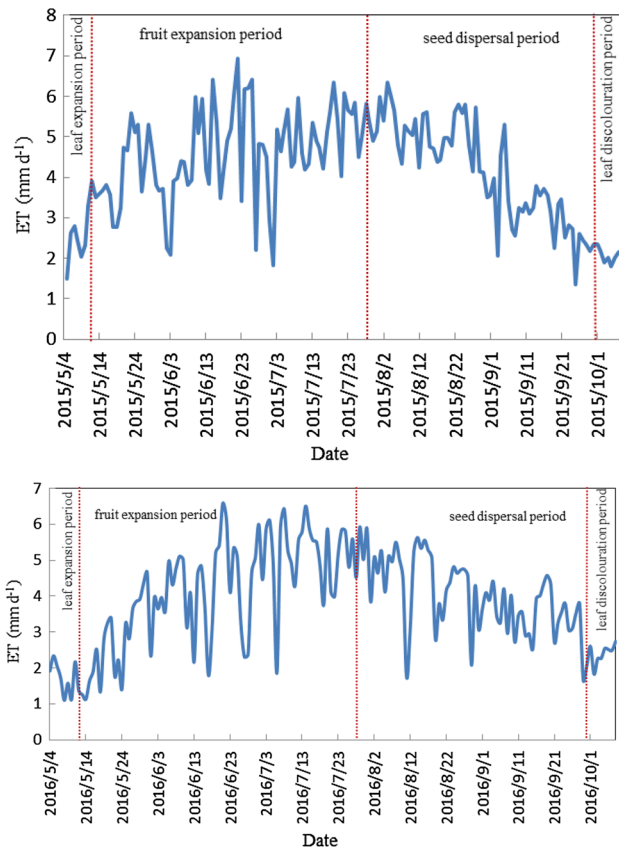


**Fig. 7** Phenological variation of evapotranspiration during the growing seasons of *Populus euphratica* in 2015 and 2016

### Comparison of the five models

Comparisons and correlations between daily estimated evapotranspiration by the five models and the measured ET by the eddy-covariant (EC) method during the 2015 and 2016 growing seasons are presented in Appendix Fig. S1 and Table 2. The  $R^2$  values of the PM model were 0.586 and 0.543, with the values of  $E_1$ ,  $d_1$  and  $M_{AE}$  at  $-1.166$ ,  $0.321$  and  $2.382$  mm in 2015, and  $-1.375$ ,  $0.357$  and  $2.340$  mm in 2016, indicating a significant overestimation. The estimates of the SW and C models were closer in agreement with the measurements, with greater values of  $R^2$ ,  $E_1$  and  $d_1$  (0.586, 0.167 and 0.542 in 2015, and 0.575, 0.162 and 0.548 in 2016

for the SW model, and 0.618, 0.288 and 0.638 in 2015, and 0.622, 0.148 and 0.624 in 2016 for the C model) and lower values of  $M_{AE}$  (0.916 in 2015 and 0.969 in 2016 for the SW model, and 0.782 in 2015 and 0.985 in 2016 for the C model) than those of the PM model. This was mainly because both models recognized the differences between  $E_s$  and  $E_c$ . Both the PT and SSW models gave the most accurate evapotranspiration values, with  $E_1$ ,  $d_1$  and  $M_{AE}$  of 0.354, 0.654 and 0.710 mm in 2015, and 0.426, 0.676 and 0.664 mm in 2016 for the PT model, and 0.321, 0.629 and 0.746 mm in 2015, and 0.433, 0.696 and 0.655 mm in 2016 for the SSW model.

### Sensitivity analysis for the SSW and PT models

Sensitivity analysis for the improved dual source (SSW) and Priestly-Taylor PT models had high accuracies for the estimation of evapotranspiration and show that both models had the greatest sensitivities to  $R_n$  (0.171 in 2015 and 0.192 in 2016 for the SSW model, and 0.214 in 2015 and 0.209 in 2016 for the PT model) (Table 3). The SSW model was also more sensitive to LAI (leaf area index) (0.090 in 2015 and 0.048 in 2016).

## Discussion

### Biotic and abiotic controls on evapotranspiration

Previous studies have shown that climate-, vegetation-, soil-related parameters, and groundwater depth are the main factors controlling evapotranspiration (Devitt et al. 2011). In this study, evapotranspiration was not only correlated to windspeed, consistent with Hao et al. (2007) and Yu et al. (2017), it was negatively correlated to volumetric water content ( $\theta$ ). The small absolute value of Pearson's correlation coefficient (0.306) revealed that soil water was not the primary water source for evapotranspiration. Groundwater, in contrast, is known to be the main source of water for *P. euphratica* forests (Si et al. 2014), and means that groundwater is a crucial factor controlling temporal patterns of evapotranspiration in riparian forests (Yu et al. 2017). Groundwater depth within 4 m was not the limiting growth factor for *P. euphratica* (Li et al. 2013). Our results show the

**Table 1** Correlations between evapotranspiration and environmental variables: net radiation ( $R_n$ ), air temperature ( $T_a$ ), vapor pressure deficit ( $D$ ), wind speed ( $u$ ), soil temperature ( $T_s$ ), groundwater depth (GWD) and soil water content ( $\theta$ ) in 2015 and 2016

Environmental variables	Year	$R_n$	$T_a$	$D$	$u$	$T_s$	GWD	$\theta$
Pearson's correlation coefficients	2015	0.803**	0.752**	0.732**	0.332*			-0.306*
	2016	0.819**	0.776**	0.721**	0.306*	0.678**	0.349*	

$R_n$  is net radiation ( $W m^{-2}$ ),  $T_a$  air temperature ( $^{\circ}C$ ),  $D$  vapor pressure deficit (kPa),  $u$  wind speed ( $m s^{-1}$ ),  $T_s$  soil temperature ( $^{\circ}C$ ), GWD groundwater depth (m),  $\theta$  soil water content (%), \* $P=0.01$ ; \*\* $P=0.001$

**Table 2** Correlation between estimated evapotranspiration by five models and measured evapotranspiration by the eddy-covariance method during the *Populus euphratica* growing seasons in 2015 and 2016

Year	Models	$E_1$	$d_1$	$M_{AE}/mm$	$R^2$	Slopes
2015	PM model	- 1.166	0.321	2.382	0.586	0.876
	PT model	0.354	0.654	0.710	0.550	0.620
	SSW model	0.321	0.629	0.746	0.655	0.616
	SW model	0.167	0.542	0.916	0.586	0.492
	C model	0.288	0.638	0.782	0.618	0.747
2016	PM model	- 1.375	0.357	2.340	0.543	0.887
	PT model	0.426	0.676	0.664	0.642	0.629
	SSW model	0.433	0.696	0.655	0.752	0.716
	SW model	0.162	0.548	0.969	0.575	0.578
	C model	0.148	0.624	0.985	0.622	0.905

$E_1$  is modified coefficient of efficiency,  $d_1$  modified index of agreement,  $M_{AE}$  mean absolute error,  $R^2$  determination coefficient, *PM* Penman–Monteith, *PT* Priestley–Taylor, *SSW* improved dual source, *SW* Shuttleworth–Wallace, *C* clumped

**Table 3** Sensitivity analysis of the improved dual source (SSW) and Priestley–Taylor (PT) models to leaf area index (LAI), net radiation ( $R_n$ ), soil heat flux ( $G$ ), vapor pressure deficit ( $D$ ) and wind speed ( $u$ ) in 2015 and 2016

Year	$S_p$	LAI	$R_n$	$G$	$D$	$u$
2015	$S_p$ (SSW)	0.090	0.171	0.007	0.016	0.028
	$S_p$ (PT)	–	0.214	0.015	–	–
2016	$S_p$ (SSW)	0.048	0.192	0.013	0.010	0.005
	$S_p$ (PT)	–	0.209	0.009	–	–

$S_p$  is sensitivity coefficient, *LAI* leaf area index,  $R_n$  net radiation  $G$  soil heat flux,  $D$  vapor pressure deficit,  $u$  wind speed, “–” indicates that the PT model was insensitive to this parameter as the formula does not incorporate it

potential water use by natural *P. euphratica* forests under a non-water stress condition, as the groundwater was always less than 3 m (Fig. 4). In addition, plant eco-physiological characteristics, especially leaf area index, are important factors affecting evapotranspiration (Fig. 5).

**Performance of the ET models**

The PM (Penman–Monteith) model always significantly overestimated evapotranspiration, similar conclusions were noted by Ortega-Farias et al. (2006) and Zhang et al. (2008). Possible reasons for this overestimation are first, extremely dry soil surfaces sharply increases surface resistance and prevents soil water from evaporating. Although total evapotranspiration slightly increased with intense solar radiation and greater vapor pressure deficit, it was lower than that determined by the meteorological variables. Surface canopy resistance in the model cannot accurately include integrated canopy and soil surface resistances. Secondly, vegetation cover of the *P. euphratica* forest is sparse and therefore did not satisfy the assumptions of the PM model. However, Li et al. (2010) concluded differently, finding that the PM model underestimated evapotranspiration. This difference may

be due to the canopy resistance and soil water state in their study; full irrigation management was performed, resulting in higher soil water levels and lower surface resistance. The Priestley–Taylor (PT) model, with an appropriately defined  $\alpha$  value, performed well despite its simplicity (Wu 2016). Several researchers have made similar conclusions (Bosveld and Bouten 2001; Summer and Jacobs 2005; Sun and Song 2008; Sentelhas et al. 2010; Ding et al. 2013). As noted previously, calibration of  $\alpha$  is important and a wide variation in this parameter has been reported. Table 4 summarizes  $\alpha$  values measured by researchers and includes our measurements. The Shuttleworth–Wallace (SW) model has been successfully applied to various crop species (Lund and Soegaard 2003; Ortega-Farias et al. 2007, 2010; Huang et al. 2020). Researchers have recently focused on improving model accuracy under specific conditions (Guan and Wilson 2009; Hu et al. 2013). In this study, the model estimated evapotranspiration highly accurately; however, it did not consider direct evaporation from the canopy, and deviations persisted. Tourula and Heikinheimo (1998) found that canopy interception accounted for 9%–14% of the total ET in a barley crop (LAI = 3.5–4.5 m<sup>2</sup> m<sup>-2</sup>). Although the leaf area index (1.9–2.4 m<sup>2</sup> m<sup>-2</sup> and 1.8–2.9 m<sup>2</sup> m<sup>-2</sup> during the

**Table 4** Values of the parameters of the Priestley–Taylor (PT) model  $\alpha$ , as measured by other studies and this research

$\alpha$	Vegetation types/Surface conditions	References
1.57	<i>Solarium tuberosum</i> L.	Jury and Tanner (1975)
1.29	Grass (soil at field capacity)	Mukammal and Neumann (1977)
1.27	Irrigated ryegrass	Davies and Allen (1973)
1.26	Saturated surface	Priestley and Taylor (1972)
1.26	Open-water surface	Priestley and Taylor (1972)
1.26	Wet meadow	Stewart and Rouse (1977)
1.21	Wet sloping grassland	Pauwels and Samson (2006)
1.18	Wet Douglas-fir forest	McNaughton and Black (1973)
1.12	Short grass	De Bruin and Holtslag (1982)
1.05	Douglas-fir forest	McNaughton and Black (1973)
1.04	Bare soil surface	Barton (1979)
1.01	Freshwater marsh	Sun and Song (2008)
0.90	Mixed reforestation (water limited)	Flint and Childs (1991)
0.87	Ponderosa pine (water limited, daytime)	Fisher et al. (2005)
0.86	<i>P. euphratica</i> forest (2015)	This study
0.84	Douglas-fir forest (unthinned)	Black (1979)
0.83	Alpine grassland (2008)	Zhu et al. (2012)
0.80	Douglas-fir forest (thinned)	Black (1979)
0.77	<i>P. euphratica</i> forest (2016)	This study
0.74	Alpine grassland (2009)	Zhu et al. (2012)
0.73	Douglas-fir forest (daytime)	Giles et al. (1984)
0.72	Spruce forest (daytime)	Shuttleworth and Calder (1979)

2015 and 2016 growing seasons, respectively) in the *P. euphratica* forest were smaller and canopies not as dense as the barley crop, canopy interception may account for a small amount of evapotranspiration. The improved dual source (SSW) model, which was more accurate than the SW model in this study and has the advantage of a simple structure requiring fewer parameters, appears more suitable to estimate evapotranspiration of these forests. However, application of the model has been rare and it needs to be tested for various vegetation types and environmental conditions. The clumped (C) model was highly complex and did not result in the best ET values because the model is difficult to parameterize and the results were vulnerable to large errors from propagating uncertainty in parameter values. Furthermore, the parameters required for the C model were available for this analysis because the study area is an intensively measured research site; other sites or large-scale modeling efforts may not be so fortunate.

The purpose for comparing the five models was to select the one most applicable to large and sparse vegetation in arid regions. By analyzing these models, the Priestley–Taylor (PT) and the improved dual source (SSW) models had the best fit, with the PT model using an appropriately defined  $\alpha$  value verified by a number of researchers, and the SSW model with its two-source structure form being suitable for sparse vegetation.

## Conclusion

Evapotranspiration of a *P. euphratica* forest was estimated using the eddy-covariance system and the Penman–Monteith, Priestly–Taylor, Shuttleworth–Wallace models, an improved dual source model, and a clumped model. Phenological variations of evapotranspiration showed single-peaked curves, while diurnal variations were not consistent due to the influence of high temperatures in the afternoons on some days. The Priestly–Taylor and the improved dual source models were more applicable than other models to extensive, sparse vegetation in extremely arid regions. The two models are highly sensitive to net radiation. Future research needs to focus on measuring evapotranspiration accurately, as well as testing and improving the models for different natural ecosystems.

**Acknowledgment** We gratefully acknowledge the valuable comments from anonymous reviewers on an earlier version of our manuscript.

## References

- Anapalli SS, Fisher DK, Pinnamaneni SR, Reddy KN (2020) Quantifying evapotranspiration and crop coefficients for cotton (*Gossypium hirsutum* L.) using an eddy covariance approach. *Agric Water Manage* 233:106091

- Barton JJ (1979) A parameterization of the evaporation from nonsaturated surfaces. *J Appl Meteorol Clim* 18:43–47
- Bastin JF, Berrahmouni N, Grainger A, Maniatis D, Mollicone D, Moore R, Patriarca C, Picard N, Sparrow B, Abraham EM, Aloui K, Atesoglu A, Attore F, Bassüllü Ç, Bey A, Garzuglia M, García-Montero LG, Groot N, Guerin G, Laestadius L, Lowe AJ, Mamane B, Marchi G, Patterson P, Rezende M, Ricci S, Salcedo I, Sanchez-Paus Diaz A, Stolle F, Surappaeva V, Castro R (2017) The extent of forest in dryland biomes. *Science* 356:635–638
- Black TA (1979) Evapotranspiration from Douglas-fir stands exposed to soil water deficits. *Water Resour Res* 15:164–170
- Bosveld FC, Bouten W (2001) Evaluation of transpiration models with observations over a Douglas-fir forest. *Agr Forest Meteorol* 108:247–264
- Comunian A, Giudici M, Landoni L, Pugnaghi S (2018) Improving Bowen-ratio estimates of evaporation using a rejection criterion and multiple-point statistics. *J Hydrol* 563:43–50
- Davies JA, Allen CD (1973) Equilibrium, potential and actual evaporation from cropped surfaces in southern Ontario. *J Appl Meteorol* 12:649–657
- De Bruin HAR, Holtslag AAM (1982) A simple parameterization of the surface fluxes of sensible and latent heat during daytime compared with the Penman-Monteith concept. *J Appl Meteorol* 21:1610–1621
- Devitt DA, Fenstermaker LF, Young MH, Conrad B, Baghzouz M, Bird BM (2011) Evapotranspiration of mixed shrub communities in phreatophytic zones of the Great Basin region of Nevada (USA). *Ecohydrology* 4:807–822
- Ding RS, Kang SZ, Li FS, Zhang YQ, Tong L (2013) Evapotranspiration measurement and estimation using modified Priestley-Taylor model in an irrigated maize field with mulching. *Agric Forest Meteorol* 168:140–148
- Dzikitia S, Volschenk T, Midgley SJE, Lötze E, Taylor NJ, Gush MB, Ntshidi Z, Zirebwa SF, Doko Q, Schmeisser M, Jarmain C, Steyn WJ, Pienaar HH (2018) Estimating the water requirements of high yielding and young apple orchards in the winter rainfall areas of South Africa using a dual source evapotranspiration model. *Agric Water Manage* 208:152–162
- Falge E, Baldocchi D, Olson R, Anthoni P, Aubinet M, Bernhofer C, Burba G, Ceulemans R, Clement R, Dolman H, Granier A, Gross P, Grünwald T, Hollinger D, Jensen NO, Katul G, Keronen P, Kowalski A, Lai CT, Law BE, Meyers T, Moncrieff J, Moors E, Munger JW, Pilegaard K, Rannik Ü, Rebmann C, Suyker A, Tenhunen J, Tu K, Verma S, Vesala T (2001) Gap filling strategies for defensible annual sums of net ecosystem exchange. *Agric Forest Meteorol* 107:43–69
- Fisher JB, De Biase TA, Qi Y, Xu M, Goldstein AH (2005) Evapotranspiration models compared on a Sierra Nevada forest ecosystem. *Environ Modell Softw* 20:783–796
- Flint AL, Childs SW (1991) Use of the Priestley-Taylor evaporation equation for soil water limited conditions in a small forest clearcut. *Agric Forest Meteorol* 56:247–260
- Gao GL, Zhang XY, Yu TF (2016a) Evapotranspiration of a *Populus euphratica* forest during the growing season in an extremely arid region of northwest China using the Shuttleworth-Wallace model. *J Forestry Res* 27:879–887
- Gao GL, Zhang XY, Yu TF, Liu B (2016b) Comparison of three evapotranspiration models with eddy covariance measurements for a *Populus euphratica* Oliv. forest in an arid region of northwestern China. *J Arid Land* 8:146–156
- Gasca-Tucker DL, Acreman MC, Agnew CT, Thompson JR (2007) Estimating evaporation from a wet grassland. *Hydrol Earth Syst Sci* 11:270–282
- Giles DG, Black TA, Spittlehouse DL (1984) Determination of growing season soil water deficits on a forested slope using water balance analysis. *Can J Forest Res* 15:107–114
- Griffis T, Sargent S, Baker J, Lee X, Tanner B, Greene J, Swiatek E, Billmark K (2008) Direct measurement of biosphere-atmosphere isotopic CO<sub>2</sub> exchange using the eddy covariance technique. *J Geophys Res-Atmos* 113:693–702
- Griffis T, Sargent S, Lee X, Baker J, Greene J, Erickson M, Zhang X, Billmark K, Schultz N, Xiao W, Hu N (2010) Determining the oxygen isotope composition of evapotranspiration using eddy covariance. *Bound-Lay Meteorol* 137:307–326
- Guan H, Wilson JL (2009) A hybrid dual source model for potential evaporation and transpiration partitioning. *J Hydrol* 377:405–416
- Hao YB, Wang YF, Huang XZ, Cui XY, Zhou XQ, Wang SP, Niu HS, Jiang GM (2007) Seasonal and interannual variation in water vapor and energy exchange over a typical steppe in Inner Mongolia, China. *Agric Forest Meteorol* 146:57–69
- Hou LG, Xiao HL, Si JH, Xiao SC, Zhou MX, Yang YG (2010) Evapotranspiration and crop coefficient of *Populus euphratica* Oliv forest during the growing season in the extreme arid region northwest China. *Agric Water Manage* 97:351–356
- Hu ZM, Yu GR, Zhou YL, Sun XM, Li YN, Shi PL, Wang YF, Song X, Zheng ZW, Zhang L, Li SG (2009) Partitioning of evapotranspiration and its controls in five grassland ecosystems: application of a two-source model. *Agric Forest Meteorol* 149:1410–1420
- Hu ZM, Li SG, Yu GR, Sun XM, Zhang LM, Han SJ, Li YN (2013) Modelling evapotranspiration by combing a two-source model, a leaf stomatal model, and a light-use efficiency model. *J Hydrol* 501:186–192
- Huang S, Yan HF, Zhang C, Wang GQ, Joe Acquah S, Yu JJ, Li LL, Ma JM, Darko RO (2020) Modeling evapotranspiration for cucumber plants based on the Shuttleworth-Wallace model in a Venlo-type greenhouse. *Agric Water Manage* 228:105861
- Juhász Á, Hrotkó K (2014) Comparison of the transpiration part of two sources evapotranspiration model and the measurements of sap flow in the estimation of the transpiration of sweet cherry orchards. *Agric Water Manage* 143:142–150
- Jung M, Reichstein M, Ciais P, Seneviratne SI, Sheffield J, Goulden ML, Bonan G, Cescatti A, Chen JQ, de Jeu R, Dolman AJ, Eugster W, Gerten D, Gianelle D, Gobron N, Heinke J, Kimball J, Law BE, Montagnani L, Mu QZ, Mueller B, Oleson K, Papale D, Richardson AD, Rouspard O, Running S, Tomelleri E, Viovy N, Weber U, Williams C, Wood E, Zaehle S, Zhang K (2010) Recent decline in the global land evapotranspiration trend due to limited moisture supply. *Nature* 467:951–954
- Jury WA, Tanner CB (1975) Advection modification of the Priestley and Taylor evapotranspiration formulae. *Agron J* 67:840–842
- Keane RE, Parsons RA, Hessburg PF (2002) Estimating historical range and variation of landscape patch dynamics: limitations of the simulation approach. *Ecol Model* 151:29–49
- Legates DR, McCabe GJ (1999) Evaluating the use of goodness-of-fit measures in hydrologic and hydroclimatic model validation. *Water Resour Res* 35:233–241
- Li XY, Yang PL, Ren SM, Li YK, Liu HL, Du J, Li PF, Wang CY, Ren L (2010) Modelling cherry orchard evapotranspiration based on an improved dual source model. *Agric Water Manage* 98:12–18
- Li W, Zhou H, Fu A, Chen Y (2013) Ecological response and hydrological mechanism of desert riparian forest in inland river, north-west of China. *Ecohydrology* 6:949–955
- Li XY, He Y, Zeng ZZ, Lian X, Wang XH, Du MY, Jia GS, Li YN, Ma YM, Tang YH, Wang WZ, Wu ZX, Yan JH, Yao YT, Ciais P, Zhang XZ, Zhang YP, Zhang Y, Zhou GS, Piao SL (2018) Spatiotemporal pattern of terrestrial evapotranspiration in China during the past thirty years. *Agric Forest Meteorol* 259:131–140
- Li XH, Farooqi TJA, Jiang C, Liu SR, Sun OJX (2019) Spatiotemporal variations in productivity and water use efficiency across a temperate forest landscape of Northeast China. *For Ecosyst* 6:22
- Liu GS, Liu Y, Hafeez M, Xu D, Vote C (2012) Comparison of two methods to derive time series of actual evapotranspiration using

- eddy covariance measurements in the southeastern Australia. *J Hydrol* 454–455:1–6
- Lu XF, Liang LY, Wang LX, Jenerette D, McCabe MF, Grantz DA (2017) Partitioning of evapotranspiration using a stable isotope technique in an arid and high temperature agricultural production system. *Agric Water Manage* 179:103–109
- Lund MR, Soegaard H (2003) Modelling of evaporation in a sparse millet crop using a two-source model including sensible heat advection within the canopy. *J Hydrol* 280:124–144
- Ma Y, Song XF (2019) Applying stable isotopes to determine seasonal variability in evapotranspiration partitioning of winter wheat for optimizing agricultural management practices. *Sci Total Environ* 654:633–642
- Maruyama T, Ito K, Takimoto H (2019) Abnormal data rejection range in the Bowen ratio and inverse analysis methods for estimating evapotranspiration. *Agric Forest Meteorol* 269–270:323–334
- Maxwell R, Condon L (2016) Connections between groundwater flow and transpiration partitioning. *Science* 353:377–380
- McNaughton KG, Black TA (1973) A study of evapotranspiration from a Douglas Fir forest using the energy balance approach. *Water Resour Res* 9:1579–1590
- Mo XG (1998) Modelling and validating water and energy transfer in soil-vegetation-atmosphere system. *Acta Meteorol Sin* 56:323–332
- Monteith JL (1965) Evaporation and atmosphere. The state and movement of water in living organisms. *Symp Soc Exp Biol* 19:205–234
- Mukammal EI, Neumann HH (1977) Application of the Priestley-Taylor evaporation model to assess the influence of soil moisture on the evaporation from a large weighing lysimeter and class A pan. *Bound-Lay Meteorol* 12:243–256
- Oki T, Kanae S (2006) Global hydrological cycles and world water resources. *Science* 313:1068–1072
- Ortega-Farias S, Olioso A, Fuentes S, Valdes H (2006) Latent heat flux over a furrow-irrigated tomato crop using Penman-Monteith equation with a variable surface canopy resistance. *Agric Water Manage* 82:421–432
- Ortega-Farias S, Carrasco M, Olioso A, Acevedo C, Poblete C (2007) Latent heat flux over Cabernet Sauvignon vineyard using the Shuttleworth and Wallace model. *Irrigation Sci* 25:161–170
- Ortega-Farias S, Poblete-Echeverría C, Brisson N (2010) Parameterization of a two-layer model for estimating vineyard evapotranspiration using meteorological measurements. *Agric Forest Meteorol* 150:276–286
- Pauwels VRN, Samson R (2006) Comparison of different methods to measure and model actual evapotranspiration rates for a wet sloping grassland. *Agric Water Manage* 82:1–24
- Peters A, Groh J, Schrader F, Durner W, Vereecken H, Pütz T (2017) Towards an unbiased filter routine to determine precipitation and evapotranspiration from high precision lysimeter measurements. *J Hydrol* 549:731–740
- Priestley CHB, Taylor RJ (1972) On the assessment of surface heat and evaporation using large-scale parameters. *Mon Weather Rev* 100:81–92
- Rafi Z, Merlin O, Le Dantec V, Khabba S, Mordelet P, Er-Raki S, Amazirh A, Olivera-Guerra L, Hssaine BA, Simonneaux V, Ezzahar J, Ferrer F (2019) Partitioning evapotranspiration of a drip-irrigated wheat crop: intercomparing eddy covariance-, sap flow-, lysimeter- and FAO-based methods. *Agric Forest Meteorol* 265:310–326
- Scott RL, Huxman TE, Cable WL, Emmerich WE (2006) Partitioning of evapotranspiration and its relation to carbon dioxide exchange in a Chihuahuan Desert shrubland. *Hydrol Process* 20:3227–3243
- Sentelhas PC, Gillespie TJ, Santos EA (2010) Evaluation of FAO Penman-Monteith and alternative methods for estimating reference evapotranspiration with missing data in Southern Ontario, Canada. *Agric Forest Meteorol* 97:635–644
- Shuttleworth WJ, Calder IR (1979) Has the Priestley-Taylor equation any relevance to forest evaporation? *J Appl Meteorol* 18:639–646
- Si JH, Feng Q, Cao SK, Yu TF, Zhao CY (2014) Water use sources of desert riparian *Populus euphratica* forests. *Environ Monit Assess* 186:5469–5477
- Spinelli GM, Snyder RL, Sanden BL, Gilbert M, Shackel KA (2017) Low and variable atmospheric coupling in irrigated Almond (*Prunus dulcis*) canopies indicates a limited influence of stomata on orchard evapotranspiration. *Agric Water Manage* 196:57–65
- Stewart RB, Rouse WR (1977) Substantiation of the Priestley and Taylor parameter  $\alpha = 1.26$  for potential evaporation in high latitudes. *J Appl Meteorol* 16:649–650
- Sturm P, Eugster W, Knohl A (2012) Eddy covariance measurements of CO<sub>2</sub> isotopologues with a quantum cascade laser absorption spectrometer. *Agric Forest Meteorol* 152:73–82
- Summer DM, Jacobs JM (2005) Utility of Penman-Monteith, Priestley-Taylor, reference evapotranspiration, and pan evaporation methods to estimate pasture evapotranspiration. *J Hydrol* 308:81–104
- Sun L, Song CC (2008) Evapotranspiration from a freshwater marsh in the Sanjiang Plain, Northeast China. *J Hydrol* 352:202–210
- Tourula T, Heikinheimo M (1998) Modelling evapotranspiration from a barley field over the growing season. *Agric Forest Meteorol* 91:237–250
- Uddin J, Hancock NH, Smith RJ, Foley JP (2013) Measurement of evapotranspiration during sprinkler irrigation using a precision energy budget (Bowen ratio, eddy covariance) methodology. *Agric Water Manage* 116:89–100
- Vickers D, Mahrt L (1997) Quality control and flux sampling problems for tower and aircraft data. *J Atmos Ocean Tech* 14:512–526
- Villagarcía L, Were A, García M, Domingo F (2010) Sensitivity of a clumped model of evapotranspiration to surface resistance parameterisations: application in a semi-arid environment. *Agric Forest Meteorol* 150:1065–1078
- Wang P, Grinevsky SO, Pozdniakov SP, Yu JJ, Dautova DS, Min LL, Du CY, Zhang YC (2014) Application of the water table fluctuation method for estimating evapotranspiration at two phreatophyte-dominated sites under hyper-arid environments. *J Hydrol* 519:2289–2300
- Wang P, Li XY, Huang YM, Liu SM, Xu ZW, Wu XC, Ma YJ (2016) Numerical modeling the isotopic composition of evapotranspiration in an arid artificial oasis cropland ecosystem with high-frequency water vapor isotope measurement. *Agric Forest Meteorol* 230–231:79–88
- Wei Z, Liu Y, Xu D, Cai JB, Zhang BZ (2013) Application and comparison of winter wheat canopy resistance estimation models based on the scaling-up of leaf stomatal conductance. *Chin Sci Bull* 58:2909–2916
- Wei ZW, Lee XH, Wen XF, Xiao W (2018) Evapotranspiration partitioning for three agro-ecosystems with contrasting moisture conditions: a comparison of an isotope method and a two-source model calculation. *Agric Forest Meteorol* 252:296–310
- Widmoser P, Wohlfahrt G (2018) Attributing the energy imbalance by concurrent lysimeter and eddy covariance evapotranspiration measurements. *Agric Forest Meteorol* 263:287–291
- Williams DG, Cable W, Hultine K, Hoedjes JCB, Yepez EA, Simonneaux V, Er-Raki S, Boulet G, de Bruin HAR, Chehbouni A, Hartogensis OK, Timouk F (2004) Evapotranspiration components determined by stable isotope, sap flow and eddy covariance techniques. *Agric Forest Meteorol* 125:241–258
- Wu HL (2016) Evapotranspiration estimation of *Platycladus orientalis* in Northern China based on various models. *J Forestry Res* 27:871–878
- Xu GP, Xue XZ, Wang P, Yang ZS, Yuan WY, Liu XF, Lou CJ (2018) A lysimeter study for the effects of different canopy sizes on

- evapotranspiration and crop coefficient of summer maize. *Agric Water Manage* 208:1–6
- Yepez EA, Williams DG, Scott RL, Lin G (2003) Partitioning overstory and understory evapotranspiration in a semiarid savanna woodland from the isotopic composition of water vapor. *Agric Forest Meteorol* 119:53–68
- Yu TF, Feng Q, Si JH, Zhang XY, Zhao CY (2017) Evapotranspiration of a *Populus euphratica* Oliv. forest and its controlling factors in the lower Heihe River Basin, Northwest China. *Sci Cold Arid Region* 9:175–182
- Yu TF, Feng Q, Si JH, Zhang XY, Xi HY, Zhao CY (2018) Comparable water use of two contrasting riparian forests in the lower Heihe River basin, Northwest China. *J Forestry Res* 29:1215–1224
- Zeggaf AT, Takeuchi S, Dehghanisanij H, Anyoji H, Yano T (2007) A Bowen ratio technique for partitioning energy fluxes between maize transpiration and soil surface evaporation. *Agron J* 100:988–996
- Zhan X, Kustas WP, Humes KS (1996) An intercomparison study on models of sensible heat flux over partial canopy surfaces with remotely sensed surface temperature. *Remote Sens Environ* 58:242–256
- Zhang Y, Munkhtsetseg E, Kadota T, Ohata T (2005) An observational study of ecohydrology of a sparse grassland at the edge of the *Eurasian cryosphere* in Mongolia. *J Geophys Res-Atmos* 110:85–90
- Zhang H, Li JQ, Li JW, Zhang YB, Sun L, Wu P, Zhao J (2007) The reproductive phenological rhythm characteristics of *Populus euphratica* Olive. population in the Ejina oasis of Inner Mongolia. *J Inner Mongolia Agric Univ* 28:60–66 (**in Chinese**)
- Zhang BZ, Kang SZ, Li FS, Zhang L (2008) Comparison of three evapotranspiration models to Bowen ration-energy balance method for a vineyard in an arid desert region of northwest China. *Agric Forest Meteorol* 148:1629–1640
- Zhu GF, Su YH, Li X, Zhang K, Li CB, Ning N (2012) Modelling evapotranspiration in an alpine grassland ecosystem on Qinghai-Tibetan plateau. *Hydrol Process* 28:610–619
- Zhu GF, Su YH, Li X, Zhang K, Li CB (2013) Estimating actual evapotranspiration from an alpine grassland on Qinghai-Tibetan plateau using a two-source model and parameter uncertainty analysis by Bayesian approach. *J Hydrol* 476:42–51
- Zhu GF, Lu L, Su YH, Wang XF, Cui X, Ma JZ, He JH, Zhang K, Li CB (2014) Energy flux partitioning and evapotranspiration in a sub-alpine spruce forest ecosystem. *Hydrol Process* 28:5093–5104

**Publisher's Note** Springer Nature remains neutral with regard to jurisdictional claims in published maps and institutional affiliations.